 CMES, vol.21, no.3, pp.193-207, 2007

Asymptotic Analysis for the Coupled Wavenumbers in an Infinite Fluid-Filled Flexible Cylindrical Shell: The Axisymmetric Mode

Abhijit Sarkar[1] **and Venkata R. Sonti**[1]

Abstract: The coupled wavenumbers of a fluid-filled flexible cylindrical shell vibrating in the axisymmetric mode are studied. The coupled dispersion equation of the system is rewritten in the form of the uncoupled dispersion equation of the structure and the acoustic fluid, with an added fluid-loading term involving a parameter ε due to the coupling. Using the smallness of Poisson's ratio (ν), a double-asymptotic expansion involving ε and ν^2 is substituted in this equation. Analytical expressions are derived for the coupled wavenumbers (for large and small values of ε). Different asymptotic expansions are used for different frequency ranges with continuous transitions occurring between them. The wavenumber solutions are continuously tracked as ε varies from small to large values. A general trend observed is that a given wavenumber branch transits from a rigid-walled solution to a pressure-release solution with increasing ε. Also, it is found that at any frequency where two wavenumbers intersect in the uncoupled analysis, there is no more an intersection in the coupled case, but a gap is created at that frequency. Only the axisymmetric mode is considered. However, the method can be extended to the higher order modes.

1 Introduction

Of the several problems in structural acoustics, wavenumber characteristics of a fluid-filled infinite flexible cylindrical shell have drawn a great deal of attention as evidenced by the related volume of work. The fluid-shell system forms a coupled waveguide in which energy propagates long distances with local exchanges occurring between the fluid and the shell. In contrast to planar fluid-structure problems, this fluid-shell system poses an additional challenge by having the motion in the three coordinate directions coupled due to the shell curvature. One common question of interest in this system is how the *in vacuo* shell wavenumbers get modified due to the presence of the fluid and also how the acoustical wavenumbers get modified when the fluid is in contact with a flexible structure. These questions have been answered through numerical simulations where individual system parameters were varied [Fuller and Fahy(1982), Pavic(1990), Cabelli(1985), Ko(1994)]. However, this numerical approach, where one chooses the fluid/structure parameters discretely and computes a single wavenumber branch, becomes laborious if one wishes to see the full character of the solution over the parameter space. Such a continuous tracking of solutions can be efficiently done using asymptotic methods.

The essence of asymptotic analysis is to arrive at a solution for a complicated system which in *some way* is near to a solvable simpler system with known analytical solutions. Using asymptotics, analytical expressions can be found for the complicated system also and these expressions are slightly modified (or perturbed) versions of those of the simpler system. This method is widely prevalent in solving for weakly nonlinear systems [Nayfeh(1985)]. Symbolic computation packages (like Maple) provide a good platform for such lengthy calculations.

Defining the fluid-loading effect in the form of a perturbation parameter, asymptotic analysis has been used to analyze structures in contact with infinite acoustic domains for plane [Morse and Ingard(1968), Crighton(1989),

[1] Facility for Research in Technical Acoustics, Department of Mechanical Engineering, Indian Institute of Science, Bangalore 560 012, India.

Sorokin(2005)] and cylindrical [Scott(1988)] geometries. In contrast, for systems with finite acoustic domains, such as a flexible acoustic duct, studies have been mainly of experimental [Huang, Choy, So and Chong(2000), Choi and Kim(2002), Au-yang(1983)] or of numerical [Fuller and Fahy(1982), Pavic(1990), Cabelli(1985), Ko(1994), Lie, Yu and Zao(2001), Pluymers, Desmet, Vandepitte and Sas(2005), Soares and Mansur(2005), Soares, Mansur and Lima(2007)] nature. Applications of the asymptotic method to finite structural-acoustic systems have not come to our notice. Recently, we have undertaken an analysis of a simple two dimensional structural acoustic waveguide system [Sarkar and Sonti(2007)].

In this study, we consider an infinite fluid-filled flexible circular cylindrical shell (see figure (1)). Our interest is to find the coupled structural acoustic wavenumbers for this system as perturbations to the uncoupled structural and acoustical wavenumbers using asymptotics. Numerical solutions to this problem have already been presented [Fuller and Fahy(1982)]. Here, we wish to bring more insight into the character of the wavenumber solutions using asymptotics. Using a fluid-loading related perturbation parameter we intend to present the full spectrum of the wavenumber solutions as this parameter is increased from zero to infinity. Only the axisymmetric mode ($n = 0$) will be considered in this study. As mentioned earlier, the inherent nature of the asymptotic method provides analytical expressions for the coupled wavenumbers in terms of the uncoupled expressions and the fluid-loading parameter.

In the following section, the uncoupled acoustic waves propagating in the infinite cylindrical duct and the structural waves in the *in vacuo* infinite cylindrical shell will be presented.

2 Uncoupled analysis

In this section, we shall derive expressions for the wavenumbers of the acoustic medium in a cylindrical shell and also the wavenumbers of an infinite cylindrical shell vibrating in vacuum. These shall be referred to as the uncoupled acoustic and structural wavenumbers, respectively. Note, the

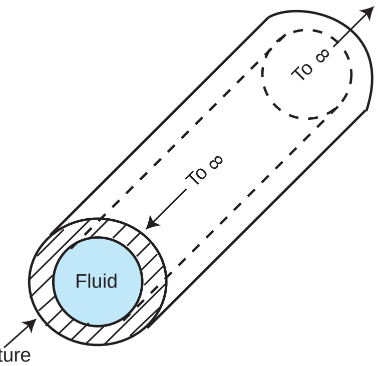

Figure 1: Schematic of the model showing the fluid-filled flexible cylindrical shell of infinite length.

uncoupled structural wavenumber is simply the *in vacuo* wavenumber. On the other hand, the uncoupled acoustic wavenumber is the wavenumber of the acoustic wave in the infinite cylindrical duct. This wavenumber depends on the acoustic boundary condition on the cylinder walls and can have two forms. The first when the cylinder wall is rigid (acoustic velocity is zero) and the second when the cylinder wall has a pressure-release condition (acoustic pressure is zero). The uncoupled acoustic wavenumber is presented in these two forms because as will be seen later, the coupled wavenumbers will turn out to be perturbations to these two forms under various situations.

In the following, we shall present derivations for the above mentioned uncoupled acoustic and structural wavenumbers at a fixed frequency ω. These derivations are available in Morse and Ingard(1968) and Fuller(1981). However, they are presented here in brief for completeness. Throughout the article a harmonic time (t) dependence of the form $e^{i\omega t}$ is assumed.

2.1 The uncoupled acoustic wavenumbers (κ_a and κ_{a0})

For the acoustic fluid, the governing equation at a frequency ω is given by

$$\nabla^2 p + \frac{\omega^2}{c_f^2} p = 0, \tag{1}$$

where p is the acoustic pressure and c_f is the sonic velocity in the acoustic fluid. Also, through the

Euler equation we have the following relation between the acoustic pressure, density of the acoustic medium (ρ_f) and the acoustic velocity ($\mathbf{v}$)

$$\nabla p = -\rho_f \frac{\partial \mathbf{v}}{\partial t}. \tag{2}$$

The ∇ and ∇^2 operators in cylindrical coordinates $(r,\ \theta, x)$ are given by [Kreyszig(1993)]

$$\begin{aligned} \nabla &\equiv \frac{\partial}{\partial r}\hat{\mathbf{e}_\mathbf{r}} + \frac{1}{r}\frac{\partial}{\partial \theta}\hat{\mathbf{e}_\theta} + \frac{\partial}{\partial x}\hat{\mathbf{e}_\mathbf{x}} \quad \text{and} \\ \nabla^2 &\equiv \frac{\partial^2}{\partial r^2} + \frac{1}{r}\frac{\partial}{\partial r} + \frac{1}{r^2}\frac{\partial^2}{\partial \theta^2} + \frac{\partial^2}{\partial x^2}, \end{aligned} \tag{3}$$

where $\hat{\mathbf{e}_\mathbf{r}}$, $\hat{\mathbf{e}_\theta}$ and $\hat{\mathbf{e}_\mathbf{x}}$ represent unit vectors in the radial, circumferential and axial directions, respectively.

Plane wave in a rigid-walled duct: For a rigid-walled duct, a solution to equation (1) of the form $Pe^{\pm i\frac{\omega}{c_f}x}$ exists for all frequencies. With $e^{i\omega t}$ convention, the plane wave traveling in the $+x$ direction is given by $Pe^{i\omega t - i\frac{\omega}{c_f}x}$. The radial velocity is zero everywhere (by equation (2)) including the duct wall. Thus, the plane wave propagates only in a rigid-walled duct.

Cut-on waves: Additionally, there are cut-on waves (with two different wall conditions specified below) which propagate beyond a cut-on frequency. In the following, we shall present a derivation for these waves for a circumferential mode of arbitrary order n and specialize to the axisymmetric mode ($n = 0$) later. To find the cut-on wave solutions, we use the method of separation of variables [Kreyszig(1993)]. We substitute $p(r,\theta,x) = R(r)X(x)\cos(n\theta)$ (this form corresponds to the n^{th} circumferential mode having n nodal diameters in the cross-section) in equation(1) to get

$$\frac{1}{R}\left(\frac{\partial^2 R}{\partial r^2} + \frac{1}{r}\frac{\partial R}{\partial r}\right) - \frac{n^2}{r^2} + \frac{1}{X}\frac{\partial^2 X}{\partial x^2} + \frac{\omega^2}{c_f^2} = 0.$$

Using separability arguments, we have

$$\begin{aligned} &\left(\frac{d^2 R}{dr^2} + \frac{1}{r}\frac{dR}{dr}\right) + \left(k_s^2 - \frac{n^2}{r^2}\right) R = 0 \\ &\Rightarrow R(r) = J_n(k_s r), \end{aligned} \tag{4a}$$

$$\text{and} \quad \frac{d^2 X}{dx^2} + k_x^2 X = 0 \Rightarrow X(x) = e^{-ik_x x}, \tag{4b}$$

where

$$k_x^2 + k_s^2 = \frac{\omega^2}{c_f^2}. \tag{4c}$$

Equation (4a) is the familiar Bessel's equation [Kreyszig(1993)] for the pressure along the radial direction, the solutions to which are the Bessel functions ($J_n(k_s r)$) and the Neumann functions ($N_n(k_s r)$) of the n^{th} order. The Neumann functions have a singularity at $r = 0$ and cannot be used for a cylindrical cavity (like the present case) where $r = 0$ is part of the domain. Thus, the wave solution (traveling in the $+x$ direction) for the acoustic pressure of the n^{th} cut-on wave is given by [Morse and Ingard(1968)]

$$p_n(r,\theta,x,t) = P_n J_n(k_s r)\cos(n\theta) e^{-ik_x x} e^{i\omega t}, \tag{5}$$

where the arbitrary constant P_n gives the amplitude.

The value of k_s in the above equation depends on the boundary condition at the cylinder wall (r=a). We consider two different boundary conditions at the wall, the rigid wall (radial velocity is zero) and the pressure release ($p = 0$). The corresponding k_s can be obtained by solving the following transcendental equations:

$J_n'(k_s a) = 0$, for a rigid-walled cylindrical duct and
$J_n(k_s a) = 0$, for a pressure release cylindrical duct.

Values for $k_s a$ for the rigid-walled and the pressure-release condition are given in Table 1 for $n = 0$. Having obtained k_s, the axial wavenumber (k_x) may be obtained by using equation (4c).

It is useful to view the radial pattern for various cases of cut-on modes. The pressure values given by $R(r) = J_0(k_s a \frac{r}{a})$ ($k_s a$ is given by Table 1) are plotted in figure (2) for the case when $n = 0$. The frequencies beyond which these modes propagate are also indicated in the figure.

In this work, we shall consider the plane wave which propagates for all frequencies in the rigid-walled cylinder and the first cut-on wave in a pressure release cylinder. The axial wavenumber (k_x)

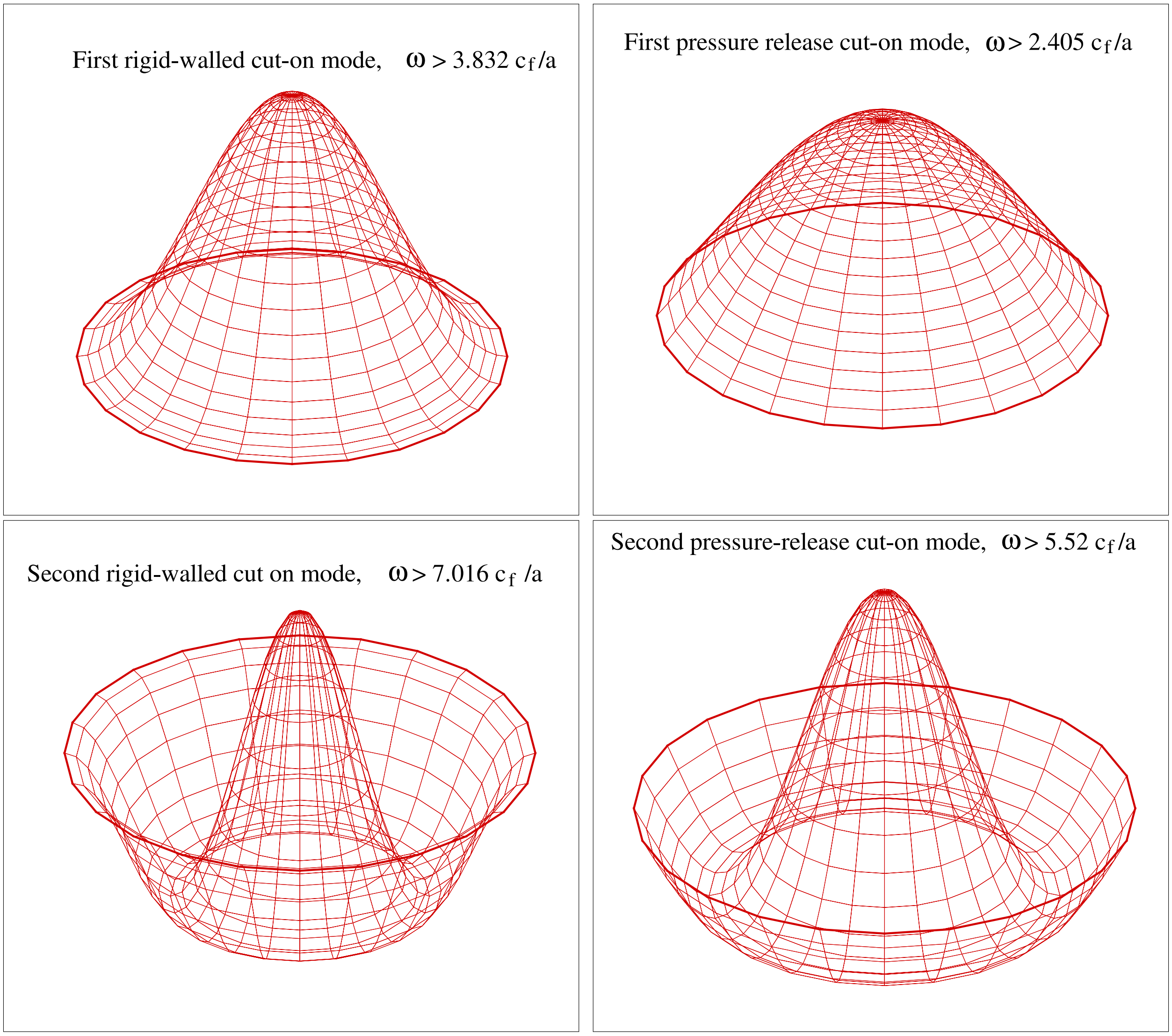

Figure 2: Cut-on acoustic modes in cylindrical duct for the axisymmetric mode ($n = 0$).

corresponding to these two waves will be denoted by κ_a and κ_{a0}, respectively. The presence of a flexible structure modifies these two uncoupled waves. In a later section, coupled wavenumbers corresponding to these two waves shall be found using asymptotics.

Table 1: $k_s a$ values for a cylindrical duct under different boundary conditions.

Mode	Rigid-walled	Pressure-release
$k_s a$	0 (plane wave)	2.405 (cut-on)

2.2 *The uncoupled structural wavenumbers ($\kappa_B(\nu)$ and $\kappa_L(\nu)$)*

The governing equations for the *in vacuo* free vibrations in the n^{th} circumferential mode, of an infinite cylindrical shell of radius a, thickness h, at a circular frequency ω are of the form

$$[L]\left\{\begin{array}{c} u_n \\ v_n \\ w_n \end{array}\right\} = \left\{\begin{array}{c} 0 \\ 0 \\ 0 \end{array}\right\}, \tag{6}$$

where u_n, v_n, w_n are the vibrational amplitudes in the axial, circumferential and radial directions, respectively and L is a matrix operator. Different shell theories have their corresponding form

Table 2: Expressions for the non-dimensional parameters in the matrix operator **L** in equation (6).

Non-dimensional Parameter	**Description**
$\beta^2 = \frac{h^2}{12a^2}$	shell thickness parameter
$\kappa = k_x a$	non-dimensional wavenumber (in the x direction), k_x being the corresponding dimensional quantity
$\Omega = \omega a / c_L$	frequency non-dimensionalized with respect to the ring frequency

for this matrix operator [Leissa(1973)]. We shall use the Donell-Mushtari theory for the cylindrical shell [Donell(1976)], where, for a shell material with density ρ_s, Poisson's ratio ν and extensional phase speed c_L, vibrating in circumferential mode n, the components of L are as follows

$$\begin{aligned} L_{11} &= -\Omega^2 + \kappa^2 + \frac{1-\nu}{2} n^2, \\ L_{22} &= -\Omega^2 + \frac{1-\nu}{2}\kappa^2 + n^2, \\ L_{33} &= -\Omega^2 + 1 + \beta^2 \left(\kappa^2 + n^2\right)^2, \\ L_{13} &= L_{31} = \nu\kappa, \\ L_{12} &= L_{21} = \frac{1}{2}(1+\nu) n\kappa, \\ L_{23} &= L_{32} = n^2. \end{aligned} \tag{7}$$

The non-dimensional terms used in the equation above are explained in Table 2.

It is apparent from the non-diagonal form of **L** that the essential complication introduced due to the shell curvature is coupling of the motions in the three perpendicular directions. The radial and circumferential directions are kinematically coupled through curvature. The axial and radial vibrations are coupled due to the Poisson's effect [Donell(1976)].

As stated earlier, we shall consider only the axisymmetric mode (*viz.* with $n = 0$). This mode is exclusively due to the extensional vibration of the shell wall and so the torsional vibration is totally uncoupled from the radial and axial vibrations. This is also seen from the form of L having L_{21}=L_{12}=L_{23}=L_{32}=0. One can find this torsional mode solution to equation (6) as $\kappa = \sqrt{\frac{2}{1-\nu}}\Omega$, propagating at a speed of $c_T = \omega/k = c_L\sqrt{(1-\nu)/2}$. Further, for this mode, it can be seen that ($u_n = w_n = 0$, $v_n \neq 0$). This mode will be excluded from further discussion in the current uncoupled analysis and eventually in the coupled analysis also.

After excluding the torsional mode, the coupled axial and radial motions may be represented by a reduced set of equations as follows

$$\begin{bmatrix} L_{11} & L_{13} \\ L_{31} & L_{33} \end{bmatrix} \left\{ \begin{array}{c} u_n \\ w_n \end{array} \right\} = \left\{ \begin{array}{c} 0 \\ 0 \end{array} \right\}, \tag{8}$$

where L_{11}, L_{13}, L_{31} and L_{33} are given by equation (7) as before. To find the free-wave solution, the determinant of the reduced matrix needs to be equated to zero. So far, in the literature, solutions to cylindrical shell waves have largely been found using either numerical techniques [Fuller(1981)] or analytical methods involving approximations [Fahy(1989)]. Below, we present the same wavenumber solutions using the asymptotic method.

Asymptotic analysis for the *in vacuo* shell wavenumbers: Using equation (7), the determinant of the reduced matrix in equation (8) can be expanded to obtain the dispersion relation as follows

$$\overbrace{\left(\kappa^2 - \Omega^2\right)}^{L} \underbrace{\left(\kappa^4 - \frac{\Omega^2 - 1}{\beta^2}\right)}_{B} - \frac{\nu^2}{\beta^2}\kappa^2 = 0, \tag{9}$$

where, $\nu^2 \ll 1$, serves as the asymptotic parameter.

With $\nu = 0$, the solution of the above dispersion relation is given by the roots of the two polynomials indicated by overbraces and underbraces. The term L has roots $\kappa = \pm\Omega$ which implies $k_x = \pm\omega/c_L$ (the longitudinal wave in the x direction), with the associated displacement in the axial direction only (*viz.* $u_n \neq 0$, $w_n = 0$). The term B in the equation (9) has the following roots

$$\kappa = \pm\sqrt[4]{\frac{\Omega^2-1}{\beta^2}}, \pm i\sqrt[4]{\frac{\Omega^2-1}{\beta^2}}, \qquad (10)$$

where, from the matrix equation (8) it is clear that the associated displacement occurs in the radial direction only (*viz.* $w_n \neq 0$, $u_n = 0$) . Also, for $\Omega \gg 1$, $\kappa \propto \sqrt{\Omega}$. Thus, this root resembles the dispersive bending (or flexural) wave solution of the plate. Henceforth, for demonstrating the asymptotic method we shall consider only the real positive roots.

With $\nu \neq 0$ such that $0<\nu^2 \ll 1$ (as is usually the case in practice), we expect solutions to equation (9) to be close to the solutions described above (with $\nu = 0$). The solution close to Ω, will be referred to as $\kappa_L(\nu)$ (L for longitudinal), while the solution close to that in equation (10) will be referred to as $\kappa_B(\nu)$ (B for bending). The solutions to (9) should be such that $\kappa_L(0) = \Omega$ and $\kappa_B(0)$ should equal that given in equation (10).

With $\nu = 0$, we have seen above that the bending and longitudinal displacements remain uncoupled. However, with $\nu \neq 0$, we no more get the associated displacement profiles to be purely longitudinal (*viz.* $w \neq 0$, $u = 0$) or purely bending (*viz.* $w \neq 0$, $u = 0$). They are still perturbations to displacement profiles with $\nu = 0$, but now due to the coupling, the displacements are dominantly longitudinal (*viz.* $u \gg w \neq 0$) and dominantly flexural (*viz.* $w \gg u \neq 0$), respectively. Using a regular perturbation method [Nayfeh(1985)], we find wavenumber solutions (given by equation 12 and 13) correct upto $\mathscr{O}(\nu^2)$. Details of the derivation are shown seperately in Box (1).

In figures (3) and (4), overlaid plots of the above solutions (*viz.* equations (12) and (13), respectively) along with the numerical solution of the dispersion equation (9) are presented. The parameters chosen are $\nu = 0.25$ and $h/a = 0.05$. Note, for the axisymmetric mode, the bending wavenumber for $\Omega < 1$ is complex (see figure (4a)) and hence the bending wave propagates only for $\Omega > 1$ [Fahy(1989)]. Also, we observe that the wavenumber for the longitudinal wave is discontinuous at $\Omega = 1$ [Fuller(1981)] (for both the asymptotic and the numerical solution).

Substituting $\kappa = k_0 + \nu^2 k_1$ in equation (9) and performing a series expansion about $\nu = 0$, we get

$$\left(k_0{}^2-\Omega^2\right)\left(k_0{}^4-\frac{\Omega^2-1}{\beta^2}\right)+\left[4\left(k_0{}^2-\Omega^2\right)k_0{}^3k_1 +2k_0k_1\left(k_0{}^4-\frac{\Omega^2-1}{\beta^2}\right)-\frac{k_0{}^2}{\beta^2}\right]\nu^2+\mathscr{O}\left(\nu^4\right)=0. \qquad (11)$$

Equating the $\mathscr{O}(1)$ term to zero we obtain the roots of k_0. It may be observed that k_0 is identical to the roots of κ with $\nu = 0$.

Putting k_0=Ω, in the equation above, at $\mathscr{O}(\nu^2)$ we get

$$k_1 = \frac{1}{2}\frac{\Omega}{\Omega^4\beta^2-\Omega^2+1}.$$

Thus, we have

$$\kappa_L(\nu) = \Omega + \frac{1}{2}\frac{\Omega\nu^2}{\Omega^4\beta^2-\Omega^2+1} + \mathscr{O}(\nu^4). \qquad (12)$$

Using $k_0 = \sqrt[4]{\frac{\Omega^2-1}{\beta^2}}$ in the $\mathscr{O}(1)$ term of equation(11) we get

$$k_1 = \frac{1}{4\beta^2\sqrt[4]{\frac{\Omega^2-1}{\beta^2}}\left(\sqrt{\frac{\Omega^2-1}{\beta^2}}-\Omega^2\right)}.$$

Thus, we have

$$\kappa_B(\nu) = \sqrt[4]{\frac{\Omega^2-1}{\beta^2}} + \frac{1}{4\beta^2\sqrt[4]{\frac{\Omega^2-1}{\beta^2}}\left(\sqrt{\frac{\Omega^2-1}{\beta^2}}-\Omega^2\right)}\nu^2 + \mathscr{O}(\nu^4). \qquad (13)$$

Box 1: Asymptotic derivation for the *in vacuo* longitudinal and flexural wavenumbers of a cylindrical shell.

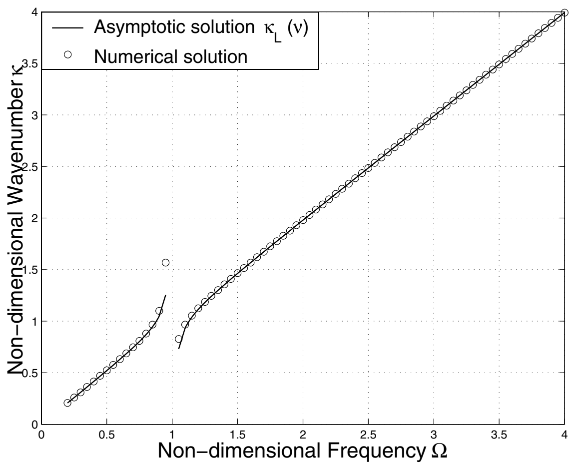

Figure 3: Wavenumber corresponding to the dominantly longitudinal mode obtained through the asymptotic method and the numerical solution for $\nu = 0.25$ and $h/a = 0.05$.

3 Formulation of the Coupled problem

The derivation of the coupled dispersion relation in a fluid-filled cylindrical shell for a general circumferential mode of order n has been presented by Fuller and Fahy(1982). In this section, we present this derivation for the sake of completeness.

For a fluid-filled cylindrical shell, the governing equation is arrived at by including the effect of the acoustic pressure as a forcing term in equation (6). Thus, we have

$$[L]\begin{Bmatrix} u_n \\ v_n \\ w_n \end{Bmatrix} = \begin{Bmatrix} 0 \\ 0 \\ \hat{p_n}(a,\theta) \end{Bmatrix}, \tag{14}$$

where $\mathbf{L}$ is given by equation (7) and $\hat{p_n}(a,\theta)$ is the acoustic pressure amplitude on the cylindrical cavity wall obtained from equation (5). Note, $p_n(a,\theta,x,t) = \hat{p_n}(a,\theta)e^{-ik_x x}e^{i\omega t}$. u_n, v_n, w_n are the vibrational amplitudes as defined in Section 2.2.

Also, at the fluid-structure interface, the acoustic velocity must equal the structural velocity in the radial direction. Using Euler equation (2), we have

$$\omega^2 \rho_f w_n = \left.\frac{\partial \hat{p_n}}{\partial r}\right|_{r=a}. \tag{15}$$

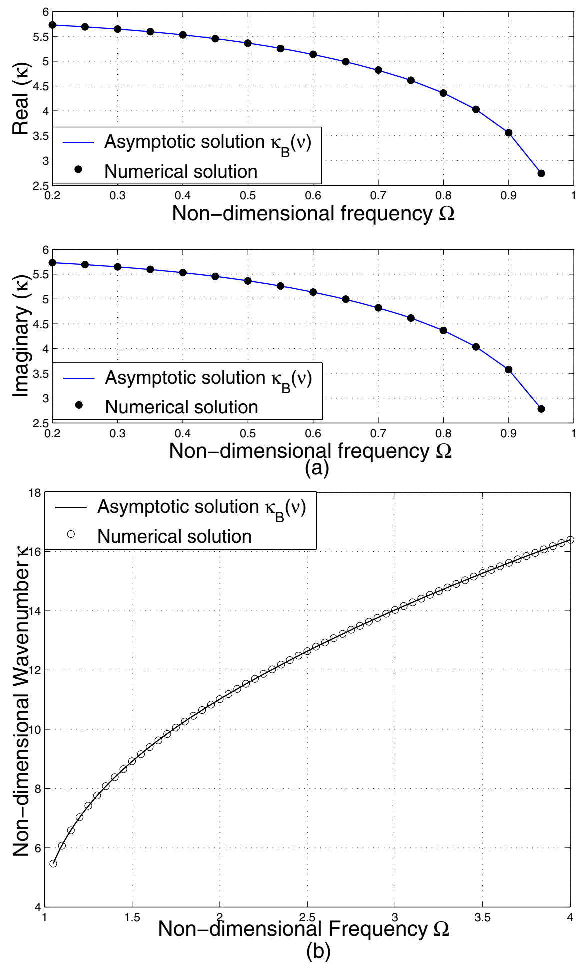

Figure 4: Wavenumber corresponding to the dominantly bending mode obtained through the asymptotic method and the numerical solution for $\nu = 0.25$ and $h/a = 0.05$. (a) Below the ring frequency ($\Omega < 1$) (b) Above the ring frequency ($\Omega > 1$).

Using the form of acoustic pressure obtained in equation (5), we get the following relation between P_n and the amplitude of radial vibration w_n

$$P_n = \frac{\omega^2 \rho_f}{k_s^r J_n'(k_s a)} w_n. \tag{16}$$

Thus, the acoustic pressure at the fluid-structure interface is given by

$$\hat{p_n}(a,\theta) = w_n \frac{\omega^2 \rho_f J_n(k_s a)}{k_s J_n'(k_s a)} \cos(n\theta). \quad (17)$$

Substituting the above relation in equation (14) we find the following governing equation for free wave propagation in a fluid-filled cylindrical shell in the n^{th} circumferential mode as

$$[L] \left\{ \begin{array}{c} u_n \\ v_n \\ w_n \end{array} \right\} = \left\{ \begin{array}{c} 0 \\ 0 \\ 0 \end{array} \right\}, \quad (18)$$

where all elements of the matrix $\mathbf{L}$ except L_{33} are given by equation (7). The L_{33} term in the equation above is modified by a fluid loading term as follows [Fuller and Fahy(1982)]

$$L_{33} = -\Omega^2 + 1 + \beta^2 \left(\kappa^2 + n^2\right)^2 - \frac{\Omega^2}{\xi} \left(\frac{\rho_f a}{\rho_s h}\right) \frac{J_n(\xi)}{J_n'(\xi)}, \quad (19)$$

where $\xi = \sqrt{\left(\frac{c_L}{c_f}\right)^2 \Omega^2 - \kappa^2}$ and $\kappa = k_x a$.

For $n=0$, as in the *in vacuo* analysis, the torsional mode ($u_n = w_n = 0$, $v_n \neq 0$) remains uncoupled (even after fluid loading) and after dropping this mode a reduced 2×2 system is obtained.

4 Solution of the coupled problem

The coupled dispersion relation for the axisymmetric mode is found by equating the determinant of $\mathbf{L}$ in equation (8) to zero with $n = 0$. Note that L_{11}, L_{13} and L_{31} are given by equation (7) and L_{33} is given by equation (19). With $J_0'(x)$=$-J_1(x)$ and upon suitably rearranging the terms we get

$$\overbrace{\left(-\Omega^2 + \kappa^2\right)}^{L} \Big[\overbrace{\left(-\Omega^2 + 1 + \beta^2 \kappa^4\right)}^{B} \overbrace{J_1(\xi)}^{R} \overbrace{\xi}^{A} + \underbrace{\Omega^2 \left(\frac{\rho_f a}{\rho_s h}\right) J_0(\xi)}_{F} \Big] - \underbrace{\nu^2 \kappa^2 J_1(\xi)\, \xi}_{P} = 0. \quad (20)$$

The physical relevance of each term in the equation above is described as follows:

- The term L equated to zero, represents the dispersion relation corresponding to the longitudinal wave in the axial direction for the *in vacuo* cylindrical shell with $\nu = 0$ $(\kappa_L(\nu), \nu = 0)$.
- The term B equated to zero, represents the dispersion relation corresponding to the flexural wave for the *in vacuo* cylindrical shell with $\nu = 0$ $(\kappa_B(\nu), \nu = 0)$.
- The term R equated to zero, represents the acoustic cut-on waves in the rigid-walled cylindrical duct.
- The term A equated to zero, represents the acoustic plane wave in the rigid-walled cylindrical duct (κ_a).
- The term P represents the Poisson's effect for the structure. We have observed earlier (see 2.2), that this can be taken into account by considering ν as a small asymptotic parameter and accurate solutions can be obtained for $0 < \nu^2 \ll 1$.
- The term F represents the effect of fluid-loading.

In equation (20), the fluid-loading effect comes from $\frac{\rho_f a}{\rho_s h}$ (the ratio of mass/area of the fluid to the structure) which will be denoted by ε. It can be seen clearly that this coupled dispersion equation is in the form of a modification (terms F and P) to the uncoupled structural dispersion equation (terms L and B) and the uncoupled acoustic dispersion equation for the rigid-walled duct (terms R and A).

We will consider the two cases $0<\varepsilon\ll 1$ and $1 \ll \varepsilon < \infty$ so that F becomes an asymptotic term, small or large. Note that P being $\mathscr{O}(\nu^2)$ is already a small asymptotic term. With this the following two cases arise:

1. When F and P are zero (*i.e.* ε and ν are zero), the roots of equation (20) are the roots of L, B, R and A. Hence, when F is of magnitude $\mathscr{O}(\varepsilon)$ $(0<\varepsilon\ll 1)$, and P is an $\mathscr{O}(\nu^2)$ term ($\nu^2 \ll 1$ in practice), the solutions should be

perturbations of the roots of L, B, R and A (*viz.* the uncoupled wavenumbers).

2. On the other hand, when $P \to 0$ (*i.e.* $\nu \to 0$) but $F \to \infty$ (*i.e.* $\varepsilon \to \infty$), the solution of equation (20) has a set of roots which approach the roots of $J_0(\xi)=0$. These roots represent the wavenumber for the pressure-release acoustic duct (the first of which is κ_{a0}). Similarly, there is the perturbation to the roots of L (the longitudinal wave), which we will not discuss further in this article.

From the previous section on uncoupled dynamics, three wavenumbers, namely κ_a and κ_{a0} and $\kappa_B(\nu)$, representing the wavenumbers of the acoustic plane wave, the first pressure-release cut-on and the *in vacuo* bending wave, respectively, were found. In the following subsections, coupled wavenumbers shall be found as perturbations to these and will be denoted by $\kappa_a(\varepsilon,\nu)$, $\kappa_{a0}(\varepsilon,\nu)$ and $\kappa_B(\varepsilon,\nu)$, respectively. The notation uses ε and ν as arguments because ε is the fluid-loading parameter and ν^2 falls out as a second perturbation parameter as in the *in vacuo* case (see the notation in Table 3). The continuous transition of the solution as ε goes from large to small values will come out from the derivations to follow.

Table 3: Notation for the uncoupled wavenumbers and the corresponding coupled wavenumbers.

Wavenumber	uncoupled	coupled
Bending wave	$\kappa_B(\nu)$	$\kappa_B(\varepsilon,\nu)$
Rigid-walled acoustic plane wave	κ_a	$\kappa_a(\varepsilon,\nu)$
First acoustic pressure release cut-on	κ_{a0}	$\kappa_{a0}(\varepsilon,\nu)$

4.1 Large ε: pressure release duct mode ($\kappa_{a0}(\varepsilon,\nu)$)

To model the effect of large ε, we make a transformation of the form $\varepsilon' = 1/\varepsilon$ in equation (20), where $0<\varepsilon'\ll 1$. This results in the following equation

$$\left(-\Omega^2+\kappa^2\right)\left[\varepsilon'\left(-\Omega^2+1+\beta^2\kappa^4\right)J_I(\xi)\xi + \Omega^2 J_O(\xi)\right] - \varepsilon'\nu^2\kappa^2 J_I(\xi) = 0. \quad (21)$$

The regular perturbation method with one small parameter was illustrated for the *in vacuo* structural solution in the earlier section. A similar approach is adopted in the present case for the two small parameters ε' and ν^2. A solution of κ in terms of the asymptotic parameters is assumed as $\kappa = k_0 + b_1\nu^2 + a_1\varepsilon'$. This is substituted in equation (21) and a double series expansion in ε' and ν is obtained. Balancing terms at $\mathscr{O}(1)$ we arrive at the following equation

$$\overbrace{(-\Omega^2+k_0^2)}^{L}\,\Omega^2 J_0\underbrace{\left(\sqrt{\left(\frac{c_L\Omega}{c_f}\right)^2 - k_0^2}\right)}_{A} = 0. \quad (22)$$

Thus, the solutions for k_0 are the *in vacuo* longitudinal wavenumber (ignoring Poisson's effect, $\kappa_L(\nu)$ at $\nu=0$) and κ_{a0} given by $J_0(A)=0$. We shall find $\kappa_{a0}(\varepsilon,\nu)$, the perturbation to κ_{a0}. Using the values given in Table 1, k_0 is given by the following equation

$$\left(\frac{c_L\Omega}{c_f}\right)^2 - k_0^2 = 2.405.^2 \quad (23)$$

At $\mathscr{O}(\varepsilon')$, we obtain the following equation

$$\left(-\Omega^2+{k_0}^2\right)\left[\left(-\Omega^2+1+\beta^2{k_0}^4\right)J_1(\xi_0)\,\xi_0 + \frac{k_0 a_1\Omega^2 J_1(\xi_0)}{\xi_0}\right] = 0, \quad (24)$$

where, k_0 is the root of equation (23) and

$$\xi_0 = \sqrt{\left(\frac{c_L}{c_f}\right)^2\Omega^2 - {k_0}^2}.$$

Thus, we have

$$a_1 = -\frac{\left(-\Omega^2+1+\beta^2{k_0}^4\right)\left[\left(\frac{c_L\Omega}{c_f}\right)^2 - k_0^2\right]}{k_0\Omega^2} \quad (25)$$

Similarly, balancing terms at $\mathscr{O}(\nu^2)$, we obtain an equation for b_1. b_1 is found to be zero. Thus, the asymptotic solution has no $\mathscr{O}(\nu^2)$ term. This is expected as in equation (21) ν^2 is multiplied by ε'. Physically, it means that the wavenumber corresponding to the pressure-release mode is mainly affected by fluid-structure coupling. The Poisson's ratio effect is much lesser.

The correction factor a_1 remains small for all frequencies except near the cut-on frequency of the first pressure-release mode. The asymptotic solution in this range is compared with the numerical solution in figure (5) for $h/a = 0.1$, $c_L/c_f = 2$, $\varepsilon = 1.25$ ($\varepsilon' = 0.8$) and $\nu = 0.25$ along with $\kappa_B(\nu)$ and κ_{a0}. As is seen from the plot, the coupled wavenumber is a perturbation to κ_{a0}.

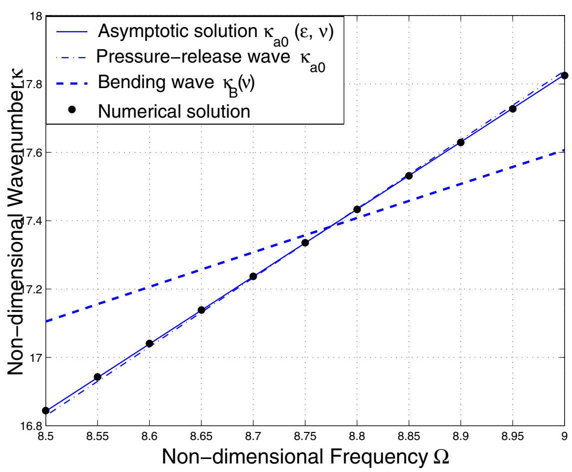

Figure 5: Coupled wavenumber solution near the first acoustic pressure-release cut-on mode for $h/a = 0.1$, $c_L/c_f = 2$, $\varepsilon = 1.25$ and $\nu = 0.25$.

The arguments given above show that for large ε the coupled wavenumber is close to the uncoupled pressure-release wavenumber. The difference between these two branches decreases with increasing ε. For the parameters chosen in figure (5), we have observed that with $\varepsilon \approx 2$, the two branches are difficult to distinguish visually. To make the distinction clear, we have chosen a *not so large* value of ε as 1.25.

Note, the sign of the perturbation (*i.e.* positive or negative) changes at the frequency where $\kappa_B(\nu)$ intersects κ_{a0}. Below this frequency, $\kappa_{a0}(\varepsilon,\nu)$ is greater than κ_{a0} and *vice-versa*. Thus, below this frequency, due to the presence of the flexible structure the compressibility of the acoustic fluid is increased and similarly decreased above this frequency.

4.2 Small ε: Bending wave and acoustic plane wave ($\kappa_B(\varepsilon,\nu)$ and $\kappa_a(\varepsilon,\nu)$)

Coincidence frequency is the frequency at which the *in vacuo* bending wavenumber equals the wavenumber of the acoustic plane wave. The asymptotic derivations in this section will consist of two separate expansions for both $\kappa_B(\varepsilon,\nu)$ and $\kappa_a(\varepsilon,\nu)$, one valid away from the coincidence frequency and the other valid near the coincidence frequency.

Away from the Coincidence frequency: For the case when $0 < \varepsilon,\ \nu^2 \ll 1$, we adopt a double asymptotic expansion method as above to obtain the solutions for the coupled dispersion equation (20). Substituting $\kappa = k_0 + a_1\varepsilon + b_1\nu^2$ in equation (20) we perform a series expansion in ε and ν. Balancing terms at $\mathscr{O}(1)$, we get the following equation for k_0

$$\left(-\Omega^2 + {k_0}^2\right)\left(-\Omega^2 + 1 + \beta^2 {k_0}^4\right) \cdot J_1\left(\sqrt{\frac{c_L}{c_f}^2 \Omega^2 - {k_0}^2}\right)\sqrt{\frac{c_L}{c_f}^2 \Omega^2 - {k_0}^2} = 0.$$

The above equation at $\mathscr{O}(1)$ carries solutions to many waves. The possible solutions for k_0 are indicated in Table 4 along with the physical nature of the solutions.

At present, we shall be interested to find the perturbations corresponding to the bending wave ($\kappa_B(\nu)$) and the acoustic plane wave (κ_a). The procedure is similar in case of other solutions. Selecting the k_0 corresponding to the bending wave (shown in Table 4), we obtain the following equa-

Table 4: $\mathscr{O}(1)$ solution for coupled wavenumbers with small fluid-loading.

$\mathbf{k_0}$	**Physical Description**
Ω	Longitudinal wave (ignoring Poisson's effect, $\kappa_L(\nu), \nu = 0$) (not discussed)
$\sqrt[4]{\frac{\Omega^2-1}{\beta^2}}$	Bending wave (ignoring Poisson's effect,$\kappa_B(\nu), \nu = 0$)
$\frac{c_L}{c_f}\Omega$	Rigid-walled acoustic plane wave κ_a
Root of $J_1(\sqrt{(c_L\Omega/c_f)^2 - k^2})$	Rigid-walled acoustic duct first cut-on (not discussed)

tion at $\mathscr{O}(\varepsilon)$

$$\left(-\Omega^2 + \frac{\sqrt{(\Omega^2-1)\beta^2}}{\beta^2}\right) \left[\Omega^2 J_0(\Theta) + 4\left(\left(\Omega^2-1\right)\beta^2\right)^{3/4} a_1 J_1(\Theta) \sqrt{c^2\Omega^2 - \frac{\sqrt{(\Omega^2-1)\beta^2}}{\beta^2}\frac{1}{\beta}}\right] = 0,$$

$$\Rightarrow a_1 = -\frac{\Omega^2\beta J_0(\Theta)}{4\Theta J_1(\Theta)\left((\Omega^2-1)\beta^2\right)^{3/4}}, \tag{26}$$

where

$$\Theta = \sqrt{\frac{(c_L/c_f)^2\Omega^2\beta^2 - \sqrt{(\Omega^2-1)\beta^2}}{\beta^2}}.$$

Similarly, at $\mathscr{O}(\nu^2)$ we obtain the following equation

$$-\sqrt{(\Omega^2-1)\beta^2}J_1(\Theta)\frac{\Theta}{\beta^2} + 4\left(-\Omega^2 + \frac{\sqrt{(\Omega^2-1)\beta^2}}{\beta^2}\right) \left(\left(\Omega^2-1\right)\beta^2\right)^{3/4} b_1 J_1(\Theta)\frac{\Theta}{\beta} = 0$$

$$\Rightarrow b_1 = -\frac{1}{4}\frac{\beta}{\sqrt[4]{(\Omega^2-1)\beta^2}\left(\Omega^2\beta^2 - \sqrt{(\Omega^2-1)\beta^2}\right)}.$$

To find the solution $\kappa_a(\varepsilon,\nu)$, we put $k_0 = c_L\Omega/c_f$. Performing a similar order balance we obtain

$$a_1 = \frac{\Omega}{\frac{c_L}{c_f}\left[-\Omega^2 + 1 + \left(\frac{c_L\Omega}{c_f}\right)^4\beta^2\right]} \text{ and } b_1 = 0.$$

Thus, the asymptotic expressions for these are given as follows.

$$\kappa_B(\varepsilon,\nu) = \sqrt[4]{\frac{\Omega^2-1}{\beta^2}} - \frac{\Omega^2\beta J_0(\Theta)\varepsilon}{4\Theta J_1(\Theta)\left((\Omega^2-1)\beta^2\right)^{3/4}} - \frac{\beta\nu^2}{4\sqrt[4]{(\Omega^2-1)\beta^2}\left(\Omega^2\beta^2 - \sqrt{(\Omega^2-1)\beta^2}\right)}, \tag{27}$$

$$\kappa_a(\varepsilon,\nu) = \Omega + \frac{\Omega}{2\left[-\Omega^2 + 1 + \left(\frac{c_L\Omega}{c_f}\right)^4\beta^2\right]}\varepsilon. \tag{28}$$

Near the Coincidence frequency: The correction factor a_1 obtained for both $\kappa_a(\varepsilon,\nu)$ and $\kappa_B(\varepsilon,\nu)$ becomes large at frequencies near the coincidence frequency (where $\kappa_B(\nu) = \kappa_a$). The coincidence frequency (Ω_c) is obtained by equating the components B and A in equation (20), for small ν^2. It follows that Ω_c and the corresponding wavenumber (κ_c) are then given by

$$\Omega_c = \sqrt{\frac{1}{2}\frac{1 + \sqrt{1 - 4\beta^2(c_L/c_f)^4}}{\beta^2(c_L/c_f)^4}}, \quad \kappa_c = \frac{c_L\Omega_c}{c_f}.$$

For solutions near the coincidence frequency, we substitute $\Omega = \Omega_c + \varepsilon\Psi$ in equation (20) (where Ψ is an $\mathscr{O}(1)$ quantity). Further simplifying assumptions are made as follows:

1. For real Ω_c (see equation above) it is required to have $\beta^2\left(\frac{c_L}{c_f}\right)^4 < \frac{1}{4}$. Thus, we may assume that for cases of practical interest $\beta^2\left(\frac{c_L}{c_f}\right)^4 \ll 1$.

2. Due to the assumption (1) above we have

$$\Omega_c \approx \sqrt{\frac{1}{2}\frac{1+\left(1-2\beta^2\frac{c_L^4}{c_f^4}\right)}{\beta^2\frac{c_L^4}{c_f^4}}}$$

$$=\sqrt{\frac{1}{2}\frac{2-2\beta^2\frac{c_L^4}{c_f^4}}{\beta^2\frac{c_L^4}{c_f^4}}}=\sqrt{\frac{c_f^4}{\beta^2 c_L^4}-1}\approx\frac{c_f^2}{\beta c_L^2}$$

   and

$$\kappa_c=\frac{c_f}{\beta c_L}.$$

3. Due to the form of Ω_c and κ_c obtained above and assumption (1), Ω_c, $\kappa_c \gg 1$. Thus, for frequencies around Ω_c the term B in equation (20) may simplified to $-\Omega^2+\beta^2\kappa^4$.

4. As we are looking for the perturbation solution of the coupled wavenumber around the coincidence frequency, κ should be such that $-\Omega^2+\beta^2\kappa^4\approx 0$ (near the wavenumber of the *in vacuo* structural bending mode) and $\kappa \approx c_L\Omega/c_f$(near the wavenumber of the acoustic plane wave).

5. Due to the latter condition in (4) above, the argument of the Bessel functions in equation (20) is small. Note, for small x, $J_0(x)\approx 1$ and $J_1(x)\approx x/2$.

6. As ν^2 is another asymptotic term, it has no effect on a_1 which is the correction term due to the asymptotic term ε. Hence, the term P in equation (20) may be neglected for evaluation of the correction factor a_1.

Using the above simplifications in equation (20) the coupled dispersion equation near the coincidence frequency reduces to

$$\frac{-\overline{\Omega}^2+\beta^2\kappa^4}{2}\left(\frac{c_L^2\overline{\Omega}^2}{c_f^2}-\kappa^2\right)+\varepsilon\overline{\Omega}^2=0,$$

where

$$\overline{\Omega}=\frac{c_f^2}{\beta c_L^2}+\varepsilon\Psi.$$

To find $\kappa_a(\varepsilon,\nu)$ we substitute κ=$(c_L/c_f)(\Omega_c+\varepsilon\Psi)$+ $a_1\sqrt{\varepsilon}$ in the equation above and perform a series expansion about ε. Balancing terms at $\mathscr{O}(\varepsilon)$ we get a_1=$\pm\frac{1}{2}$. Similarly, to find $\kappa_B(\varepsilon,\nu)$ substitute κ=$\sqrt{(\Omega_c+\varepsilon\Psi)/\beta}$+$a_1\sqrt{\varepsilon}$ and repeat the process of order balance to get a_1=$\pm\frac{1}{2}$.

To choose the appropriate sign of a_1 in the above two cases we use a continuity argument. For $\Omega<\Omega_c$, but sufficiently far from Ω_c, the correction term for $\kappa_a(\varepsilon,\nu)$ (as given in equation (28)) is negative and similarly for Ω sufficiently greater than Ω_c, $\kappa_a(\varepsilon,\nu)$ is positive. Thus, for continuity it is required to have a_1=$-1/2$ when $\Omega\approx<\Omega_c$ while for $\Omega\approx>\Omega_c$, a_1=$1/2$. In case of $\kappa_B(\varepsilon,\nu)$, similarly, a_1=$1/2$ when $\Omega\approx<\Omega_c$ and for $\Omega\approx>\Omega_c$ we have $a_1=-1/2$. Thus, the coupled acoustic wavenumber branch below Ω_c continues as the coupled bending wavenumber beyond Ω_c while the coupled bending wavenumber below Ω_c continues as the wavenumber of the coupled acoustic plane wave. Each branch encounters a jump at Ω_c. This, phenomenon was also reported by earlier workers [Fuller and Fahy(1982), Cabelli(1985)].

The asymptotic solution obtained is compared with the numerical solution in figures (6), (7) and (8) (showing separate frequency ranges). The parameter values are h/a=0.1, c_L/c_f=2, ε=0.2 and $\nu=0.25$. As seen from the figures, a continuous transition is seen across the frequency ranges.

The results below the coincidence are presented from $\Omega=6$ onwards, for the sake of clarity. Even though not shown, the match is good from $\Omega=1$ and above. The above coincidence region is plotted till the frequency at which the $\kappa_B(\nu)$ equals the wavenumber of the first rigid-walled acoustic duct cut-on. At this frequency again a coincidence-like phenomenon happens with the first cut-on mode instead of the plane wave [Fuller and Fahy(1982)]. In this range a_1 as given in equation (**??**) becomes large. An alternative asymptotic expansion can be found for this range.

4.3 A branch greater than $\kappa_B(\nu)$ and κ_a

For the easier case of plate geometry, Fahy(1989) has proved that there exists a coupled wavenum-

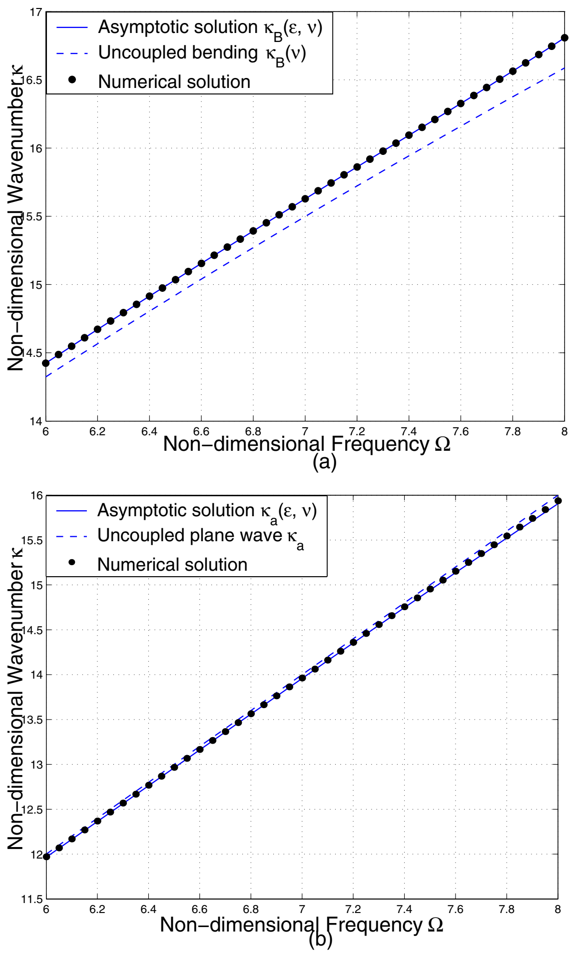

Figure 6: Coupled wavenumber solution below the coincidence frequency (Ω_c) for the fluid-filled infinite cylindrical shell with h/a=0.1, c_L/c_f=2, ε=0.2 and $\nu = 0.25$, vibrating in the axisymmetric mode (a) for the bending wave (b) for the acoustic plane wave.

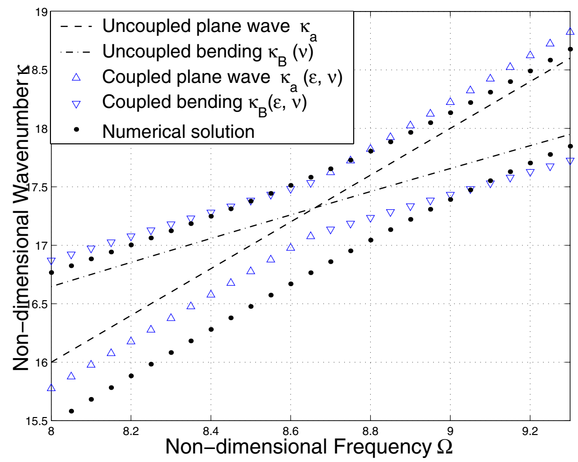

Figure 7: Coupled wavenumber solution near the coincidence frequency for the fluid-filled infinite cylindrical shell with h/a=0.1, c_L/c_f=2, ε=0.2 and $\nu = 0.25$, vibrating in the axisymmetric mode.

ber branch greater than the bending wavenumber and the wavenumber of the acoustic plane wave for all values of the fluid-loading parameter. As described in Section 4.2, we have been able to find the asymptotic expressions corresponding to this branch for small values of ε. However, for the case of large ε we could not find the asymptotic expressions corresponding to this branch. It was numerically verified that such a branch exists. The asymptotic solution is rendered difficult because this branch does not arise as perturbations to the roots of equation (21) with $\varepsilon' = 0$.

However, an intuitive argument can be given to establish the existence of such a branch. From the small ε analysis, we observed that there is a coupled wavenumber branch greater than $\kappa_B(\nu)$ and κ_a. Further, as ε increases, the difference between the coupled and the uncoupled branches increases. Thus, due to the continuous dependence of the coupled wavenumber solutions on the fluid-loading parameter, there exists a solution branch greater than the *in vacuo* bending wavenumber and the wavenumber of the acoustic plane wave for all values of the fluid-loading parameter.

To argue physically, we know that at higher frequencies the wavelength decreases. In case the wavelength is lesser than the shell curvature, it is expected that the shell behaviour will approach that of a plate of identical thickness. This was also borne out from our *in vacuo* analysis in Section 2.2. Thus, we may extend Fahy's argument for plates to high frequency waves in cylindrical geometry.

5 Conclusions

The relation of the coupled wavenumbers to the *in vacuo* bending wavenumber and the uncoupled acoustic wavenumbers (planewave and both types

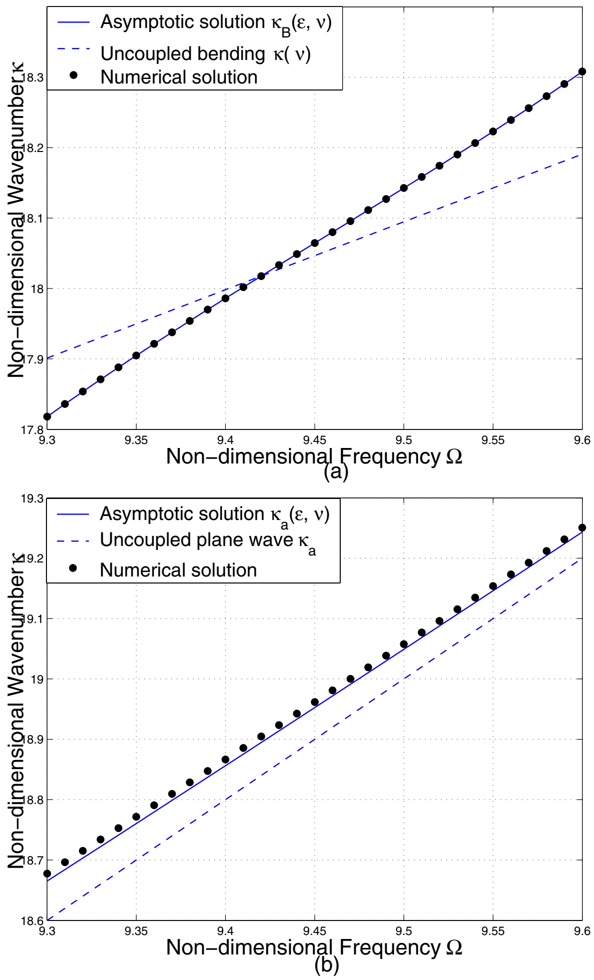

Figure 8: Coupled wavenumber solution above the coincidence frequency (Ω_c) for the fluid-filled infinite cylindrical shell with h/a=0.1, c_L/c_f=2, ε=0.2 and $\nu = 0.25$, vibrating in the axisymmetric mode (a) for the bending wave (b) for the acoustic plane wave.

of cut-on waves) is established using asymptotics. A schematic of the results found is presented in figure (9). For small ε, the coupled wavenumbers are perturbations to the *in vacuo* bending wavenumber and the wavenumbers of the rigid-walled acoustic duct (the plane wave and the cut-on). At the coincidence frequency, the branches corresponding to the coupled bending wave join with that of the coupled acoustic plane wave and *vice versa*. With increasing ε, the perturbations increase until for large values the coupled wavenumbers can be better identified as perturbations to the pressure-release acoustic cut-on wavenumbers. However, for all values of ε there is a solution of the coupled wavenumber which is greater than the *in vacuo* bending wavenumber and also the wavenumber of the acoustic plane wave. This branch for large ε, though indicated in the schematic result, has not been discussed in the article (it can be found numerically). The derivations presented can be used to continuously track the coupled wavenumber solutions from small to large ε values. Even a first order asymptotic expansion matched well with the numerical results. Results for the axisymmetric mode were presented. However, the method is applicable for higher order modes also.

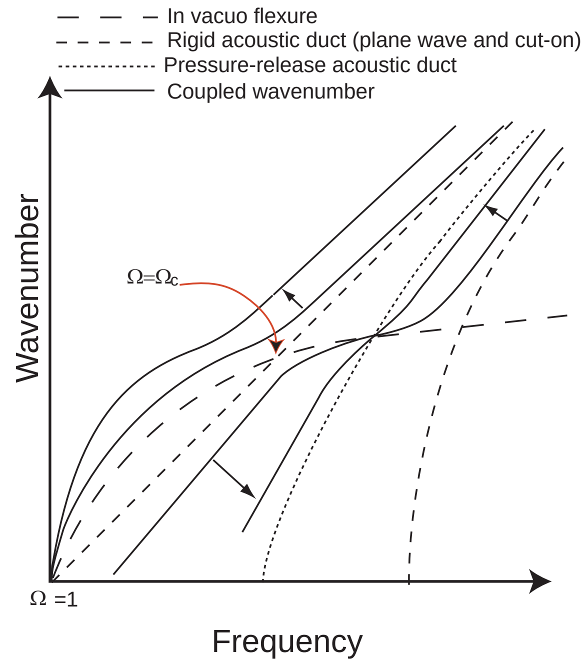

Figure 9: Schematic of the coupled wavenumber solutions. Arrows indicate the transition of solutions as ε increases.

References

Au-Yang, M. K. (1983): The hydrodynamic mass at frequencies above coincidence. *Journal of Sound and Vibration*, vol. 86, no. 2, pp. 88-292.

Cabelli, A. (1985): The propagation of sound in a square duct with non-rigid side wall. *Journal of*

Sound and Vibration, vol. 103, no. 3, pp. 379-394.

Chapman, C. J.; Sorokin, S. V. (2005): The forced vibration of an elastic plate under significant fluid loading. *Journal of Sound and Vibration*, vol. 281, pp. 719-741.

Choi, S.; Kim, Y. H. (2002): Sound wave propagation in a membrane duct. *Journal of the Acoustical Society of America*, vol. 112, no.5, pp. 1749-1752.

Crighton, D. G. (1989): The 1988 Rayleigh Medal Lecture: Fluid loading- the interaction between sound and vibration. *Journal of Sound and Vibration*, vol. 133, no. 1, pp. 1-27.

Donell, L. H. (1976): *Beams, Plates and Shells*, McGraw Hill.

Fahy, F. J. (1989) : *Sound Structure and their Interaction: Radiation*, Transmission and Response, Academic Press.

Fuller, C. R. (1981): The effect of wall discontinuities on the propagation of flexural waves in cylindrical shell. *Journal of Sound and Vibration*, vol. 75, no.2, pp. 207-228.

Fuller, C. R.; Fahy, F. J. (1982): Characteristics of wave propagation energy distributions in cylindrical elastic shells filled with fluid. *Journal of Sound and Vibration*, vol. 81, no. 4, pp. 501-518.

Huang, L.; Choy, Y. S.; So, R. M. C.; Chong, T. L. (2000): Experimental Study of sound propagation in flexible duct. *Journal of the Acoustical Society of America*, vol. 108, no. 2, pp. 625-631.

Ko, S. H. (1994): Sound wave propagation in a two dimensional flexible duct in the presence of an inviscid flow. *Journal of Sound and Vibration*, vol. 175, no. 2, pp. 279-287.

Kreyszig, E. (1993): *Advanced Engineering Mathematics, seventh edition*, John-Wiley & Sons.

Leissa, A. W. (1973): Vibration of Shells, *NASA Technical Report*, NASA SP-288.

Lie, S. T.; Yu, G.; Zhao, Z. (2001): Coupling of BEM/FEM for time domain structural-acoustic interaction problems. *CMES: Computer Modeling in Engineering and Sciences*, vol. 2, no. 2, pp. 171-182.

Morse, P. M.; Ingard, K. U. (1968): *Theoretical Acoustics*, McGrawHill Book Company.

Nayfeh, A. H. (1985): *Problems in Perturbation*, John Wiley & Sons.

Pavic, G. (1990): Vibrational energy flow in elastic circular cylindrical shell. *Journal of Sound and Vibration*, vol. 142, no. 2, pp. 293-310.

Pluymers, B.; Desmet, W.; Vandepitte, D.; Sas, P. (2005): On the use of wave-based prediction technique for steady-state structural acoustic radiation analysis. *CMES: Computer Modeling in Engineering and Sciences*, vol. 7, no. 2, pp. 173-184.

Sarkar, A.; Sonti, V. R. (2007): An asymptotic analysis for the coupled dispersion characteristics of a structural acoustic waveguide. *Journal of Sound and Vibration*, vol. 306, 2007, pp. 657-674.

Scott, J. F. M. (1988): The free modes of propagation of an infinite fluid-loaded thin cylindrical shell. *Journal of Sound and Vibration*, vol. 125, no. 2, pp. 241-280.

Soares Jr., D.; Mansur, W. J. (2005): An efficient time-domain BEM/FEM coupling for acoustic-elastodynamic interaction problems. *CMES: Computer Modeling in Engineering and Sciences*, vol. 8, no. 2, pp. 153-164.

Soares Jr., D.; Mansur W. J.; Lima, D. L. (2007): An explicit multi-level time-step algorithm to model the propagation of interacting acoustic-elastic waves using finite element/ finite difference coupled procedures. *CMES: Computer Modeling in Engineering and Sciences*, vol. 17, no. 1, 2007, pp. 19-34.